**Science & Technology Indonesia**
**p-ISSN: 2580-4405 e-ISSN: 2580-4391**
*Sci. Technol. Indonesia 2 (2017) 50-55*

Science & Technology Indonesia

*Article* http://sciencetechindonesia.com

# SYNTHESIS AND CHARACTERIZATION OF METAL OXIDES SUPPORTED KEGGIN TYPE POLYOXOMETALATE $Rb_2K_2[\gamma\text{-}H_2SiV_2W_{10}O_{40}].nH_2O$

Eiffel Ostan Jeski Gultom[1*], Aldes Lesbani[1]

[1]*Department of Chemistry, Faculty of Mathematic and Natural Sciences, Sriwijaya University*
**Corresponding Author Email: eiffelgultom@gmail.com*

## ABSTRACT

Synthesis of material based on polyoxometalate $Rb_2K_2[\gamma\text{-}H_2SiV_2W_{10}O_{40}].nH_2O$ with $SiO_2$, $TiO_2$, $ZrOCl_2$, and $TaCl_5$ was carried out to form $Rb_2K_2[\gamma\text{-}H_2SiV_2W_{10}O_{40}].nH_2O\text{-}SiO_2$, $Rb_2K_2[\gamma\text{-}H_2SiV_2W_{10}O_{40}].nH_2O\text{-}TiO_2$ $Rb_2K_2[\gamma\text{-}H_2SiV_2W_{10}O_{40}].nH_2O\text{-}ZrOCl_2$ and $Rb_2K_2[\gamma\text{-}H_2SiV_2W_{10}O_{40}].nH_2O\text{-}TaCl_5$. Materials from preparation were characterized through functional group analysis using FT-IR spectrophotometer, crystallinity analysis using XRD and surface photograph analysis using SEM. The results show that material $Rb_2K_2[\gamma\text{-}H_2SiV_2W_{10}O_{40}].nH_2O$ was successfully loaded with $SiO_2$, $ZrOCl_2$ and $TaCl_5$. Based on SEM photo $Rb_2K_2[\gamma\text{-}H_2SiV_2W_{10}O_{40}].nH_2O\text{-}TiO_2$ and $Rb_2K_2[\gamma\text{-}H_2SiV_2W_{10}O_{40}].nH_2O\text{-}ZrOCl_2$ were the best material from preparation base on the homogeneity particle distribution. The FT-IR spectrum shows specific wavenumber for nanomaterial $Rb_2K_2[\gamma\text{-}H_2SiV_2W_{10}O_{40}].nH_2O\text{-}TiO_2$ in the range 455-910 $cm^{-1}$ and $Rb_2K_2[\gamma\text{-}H_2SiV_2W_{10}O_{40}].nH_2O$ - $ZrOCl_2$ in the range 393.48-1404 $cm^{-1}$. XRD pattern for material $Rb_2K_2[\gamma\text{-}H_2SiV_2W_{10}O_{40}].nH_2O\text{-}TiO_2$ and $Rb_2K_2[\gamma\text{-}H_2SiV_2W_{10}O_{40}].nH_2O\text{-}ZrOCl_2$ show there is a difference between polyoxometalate $Rb_2K_2[\gamma\text{-}H_2SiV_2W_{10}O_{40}].nH_2O$, $TiO_2$ and $ZrOCl_2$. SEM photo analysis of $Rb_2K_2[\gamma\text{-}H_2SiV_2W_{10}O_{40}].nH_2O\text{-}TiO_2$ and $Rb_2K_2[\gamma\text{-}H_2SiV_2W_{10}O_{40}].nH_2O\text{-}ZrOCl_2$ showed that material polyoxometalate with support has a diameter size of particle above 100 nm.

**Keywords**: $Rb_2K_2[\gamma\text{-}H_2SiV_2W_{10}O_{40}].nH_2O$, polyoxometalate, $SiO_2$, $TaCl_5$, $TiO_2$, $ZrOCl_2$.

## INTRODUCTION

Synthesis, modification, and preparation of inorganic material are still developed until this year. Various inorganic materials such as metal oxides (Wang et.al, 2017), zeolites (Dehghan and Anbia, 2017), layer materials (Hanifa and Palapa, 2016), inorganic complexes (Ramdass et.al, 2017), organometallic compounds (Pettinari, et.al, 2016) are widely used in many aspects of our life. These materials are also essential for an industrial processes such as catalysts, ion exchanges, membranes, adsorbents, and sensors. Among these materials, inorganic cluster such as polyoxometalates compounds is another class of unique and specific material due to the acid base and redox properties (Genovese and Lian, 2017). Polyoxometalates are metal-oxygen inorganic clusters with high adicity properties, redox properties, and high solubility due to the flexibility of metal exchange of heteroatom and addenda atom. Polyoxometalates have several structures such as Keggin, Dawson, Anderson, and also Lacunary polyoxometalates (Gao et.al, 2017). On the other hand, this material is important for industrial catalysis and has been applied in industrial organic synthesis and transformation of various functional groups. Thus the development of this material is still developed until this decade.

The developing of polyoxometalates can be reached by addenda/heteroatom metal exchange to form novel polyoxometalates or modification such as grafting (Yong et.al, 2016), sol-gel (Tambunan and Mohadi, 2017), or impregnation by other metal oxides (Dizaji et.al, 2017). The aim of these research is to obtain polyoxometalates with high acidity properties, high surface area, and low morphology size. Thus application as a catalyst for many organic reactions can be facile. Metal oxides were used as support for polyoxometalate in order to obtain high surface area and low morphology properties such as titanium, silica, and alumina. This modification method is an easy and simple way to get advantage properties of polyoxometalates.

In this research, various metal oxides such as silica, titanium, zirconium, and tantalum have been used as a support of polyoxometalate $Rb_2K_2[\gamma\text{-}H_2SiV_2W_{10}O_{40}].nH_2O$. Polyoxometalate $Rb_2K_2[\gamma\text{-}H_2SiV_2W_{10}O_{40}].nH_2O$ is vanadium substituted Keggin type polyoxometalate. We expected that modification of this polyoxometalate could obtain unique properties of this material. Polyoxometalate $Rb_2K_2[\gamma\text{-}H_2SiV_2W_{10}O_{40}].nH_2O$ supported silica, titanium, zirconium, and tantalum was characterized using FTIR spectroscopy, powder X-Ray analysis and identification of surface morphology by SEM.

## EXPERIMENTAL SECTION

### Materials and Equipment

Chemicals were used in this research from Merck and Sigma Aldrich such as sodium metasilicate, sodium tungstate, hydrochloric acid, potassium chloride, potassium carbonate, sodium metavanadate, rubidium chloride, cyclohexane, acetone, etanol, ammonia, silica dioxide, titanium dioxide, zirconium oxo chloride, and tantalum pentachloride.

FTIR spectrum was recorded using Shimadzu FTIR Prestige-21 using KBr pellet and scanning wavenumber from 300-4000 $cm^{-1}$. XRD powder pattern was obtained from Shimadzu LabX type-6000 with scanning speed one deg.$min^{-1}$. SEM photograph was obtained from SEM Jeol JED-2300.

*Article History*
Received: 21 November 2016
Received in revised form: 22 January 2017
Accepted: 3 February 2017

DOI: 10.26554/sti.2017.2.2.50-55

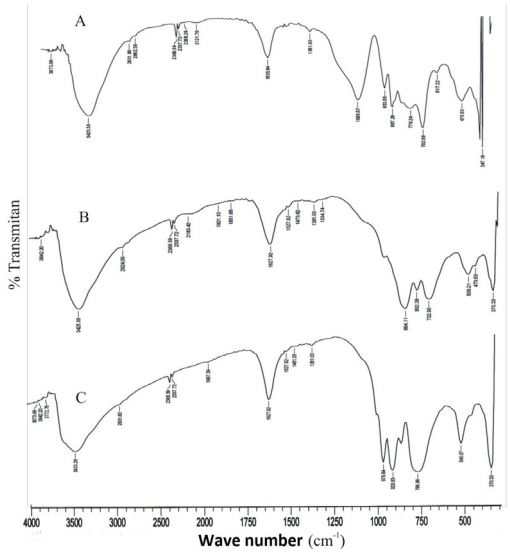


Figure 1. FTIR spectrum of $K_8[\beta_2\text{-}SiW_{11}O_{39}].14H_2O$ (A), $K_8[\gamma\text{-}SiW_{11}O_{39}].14H_2O$ (B) and $Rb_2K_2[\gamma\text{-}H_2SiV_2W_{10}O_{40}].nH_2O$ (C).

**Synthesis $Rb_2K_2[\gamma\text{-}H_2SiV_2W_{10}O_{40}].nH_2O$ (Nakagawa et.al, 2005)**

Polyoxometalate $Rb_2K_2[\gamma\text{-}H_2SiV_2W_{10}O_{40}].nH_2O$ was synthesis from $K_8[\beta_2\text{-}SiW_{11}O_{39}]14H_2O$. Sodium metavanadate 0.5 M was obtained by dissolving sodium meta vanadate in hot water (solution A). Polyoxometalate $K_8[\beta_2\text{-}SiW_{11}O_{39}]14H_2O$ (10 g) was mixed with 35 mL of hydrochloric acid 1M (solution B). Solution A was added quickly to solution B with gentle stirring and the solution to be yellow. Into these solutions, rubidium chloride (5) was added, and the solution was mixed for 15 minutes to form yellow crystals. Yellow crystals were vacuum filtered. The crystals were dissolved in water, and remaining crystals were removed by filtration. The solution was vacuum concentrated to form yellow crystals of $Rb_2K_2[\gamma\text{-}H_2SiV_2W_{10}O_{40}].nH_2O$. Characterization was conducted using FTIR, XRD, and SEM analyses.

**Preparation of $Rb_2K_2[\gamma\text{-}H_2SiV_2W_{10}O_{40}].nH_2O/SiO_2$ (Kim et.al, 2006)**

Polyoxometalate $Rb_2K_2[\gamma\text{-}H_2SiV_2W_{10}O_{40}].nH_2O$ (1g) was dissolved with 50 mL methanol. Silica dioxide (2.5 g, 24o mesh) was added into polyoxometalate solution and solution was stirred for 30 minutes. The solution was kept for 24 hours and concentrated by vacuum. The solid material was washed with acetone and dried at 110 $^oC$.

**Preparation of $Rb_2K_2[\gamma\text{-}H_2SiV_2W_{10}O_{40}].nH_2O/TiO_2$ (Pozniczek et al. 2006)**

Preparation of $Rb_2K_2[\gamma\text{-}H_2SiV_2W_{10}O_{40}].nH_2O/TiO_2$ was carried out with slight modification from Pozniczek. Titanium oxide (1 g) was mixed with ethanol (50 mL) and into the solution was added $Rb_2K_2[\gamma\text{-}H_2SiV_2W_{10}O_{40}].nH_2O$ (1g). The solution was heated at 50 $^oC$ for 45 minutes. The solid material was formed after cooling solution and was washed with acetone. Material was dried at 110 $^oC$ for 24 hours to form $Rb_2K_2[\gamma\text{-}H_2SiV_2W_{10}O_{40}].nH_2O/TiO_2$

**Preparation of $Rb_2K_2[\gamma\text{-}H_2SiV_2W_{10}O_{40}].nH_2O/ZrOCl_2$ (Devassy et al. 2002)**

Procedure for preparation of $Rb_2K_2[\gamma\text{-}H_2SiV_2W_{10}O_{40}].nH_2O/ZrOCl_2$ was adopted from Devassy and was modified as follow. Polyoxometalate $Rb_2K_2[\gamma\text{-}H_2SiV_2W_{10}O_{40}].nH_2O$ (1g) was dissolved in methanol (10 mL) (solution A). Zirconium oxo chloride (2.5 g) was mixed with ammonia (10 mL) (solution B). Solution A was mixed with solution B with slowly stirring at 50 $^oC$ for 15 minutes. The solution was centrifuged at 15,000 rpm for 5 minutes to form the solid material of $Rb_2K_2[\gamma\text{-}H_2SiV_2W_{10}O_{40}].nH_2O/ZrOCl_2$. Materi $Rb_2K_2[\gamma\text{-}H_2SiV_2W_{10}O_{40}].nH_2O/TaCl_5$ al was washed with acetone and dried at 110 $^oC$ for 24 hours.

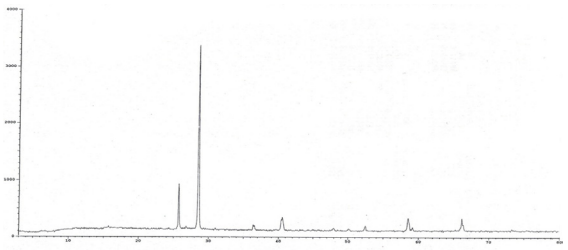

Figure 2. XRD powder pattern of $Rb_2K_2[\gamma\text{-}H_2SiV_2W_{10}O_{40}].nH_2O$.

**Preparation of $Rb_2K_2[\gamma\text{-}H_2SiV_2W_{10}O_{40}].nH_2O/TaCl_5$ (Xu et al. 2008)**

Polyoxometalate $Rb_2K_2[\gamma\text{-}H_2SiV_2W_{10}O_{40}].nH_2O$ (0.5 g) was dissolved in ethanol (4 mL) and water (2 mL) was added into these solutions (solution A). Tantalum pentachloride (0.6 g) was mixed with ethanol (5 mL) (solution B). Solution B was mixed with solution A with slowly stirring for 1 hour. The solution was kept for 30 oC overnight to form gel. Gel was heated at 130 oC for 1 hour to form a solid material of $Rb_2K_2[\gamma\text{-}H_2SiV_2W_{10}O_{40}].nH_2O/TaCl_5$. The material was kept at 110 oC overnight to obtain $Rb_2K_2[\gamma\text{-}H_2SiV_2W_{10}O_{40}].nH_2O/TaCl_5$.

Characterization of metal oxides supported $Rb_2K_2[\gamma\text{-}H_2SiV_2W_{10}O_{40}].nH_2O$. Characterization of metal oxides supported polyoxometalate was carried out using the identification of functional groups by FTIR, X-Ray powder analysis, and surface morphology analysis by SEM.

## RESULTS AND DISCUSSION

Polyoxometalate $Rb_2K_2[\gamma\text{-}H_2SiV_2W_{10}O_{40}].nH_2O$ was synthesized from polyoxometalates $K_8[\beta_2\text{-}SiW_{11}O_{39}].14H_2O$ and $K_8[\gamma\text{-}SiW_{11}O_{39}].14H_2O$, thus comparison of FTIR spectrum of these compounds is needed as shown in Figure 1. Figure 1 shows FTIR spectrum of $K_8[\beta_2\text{-}SiW_{11}O_{39}].14H_2O$ (A), $K_8[\gamma\text{-}SiW_{11}O_{39}].14H_2O$ (B) and $Rb_2K_2[\gamma\text{-}H_2SiV_2W_{10}O_{40}].nH_2O$ (C). All these Keggin type polyoxometalates have a similar vibration at wavenumber in the range 700-1100 $cm^{-1}$. The main vibration of these polyoxometalate is Si-O (at 700-720 $cm^{-1}$), W-Oc-W and W-Oe-W (at 800-880 $cm^{-1}$), and W=O (at 900-920 $cm^{-1}$) (Nakagawa and Mizuno, 2007). Wavenumber at 3300 $cm^{-1}$ is appeared in all FTIR spectra in Figure 1 due to water content. There are no significant changes in vibration of these three polyoxometalates. Thus polyoxometalate $Rb_2K_2[\gamma\text{-}H_2SiV_2W_{10}O_{40}].nH_2O$ is characterized using X-ray analysis.

Polyoxometalate $Rb_2K_2[\gamma\text{-}H_2SiV_2W_{10}O_{40}].nH_2O$ were analyzed using X-ray analysis as shown in Figure 2. There are sharp diffraction peaks at 2θ value 26 deg, and 28 deg, which is contributed from crystalline substituted Keggin polyoxometalate. Furthermore, polyoxometalate $Rb_2K_2[\gamma\text{-}H_2SiV_2W_{10}O_{40}].nH_2O$ was identified by SEM to know the morphology of these compound as shown in Figure 3.

Figure 3 showed that polyoxometalate $Rb_2K_2[\gamma\text{-}H_2SiV_2W_{10}O_{40}].nH_2O$ has a uniform with block shape. The particle size of $Rb_2K_2[\gamma\text{-}H_2SiV_2W_{10}O_{40}].nH_2O$ can be determined from Figure 3. The results show compound $Rb_2K_2[\gamma\text{-}H_2SiV_2W_{10}O_{40}].nH_2O$ has particle size distribution 1000 nm. This results indicated that

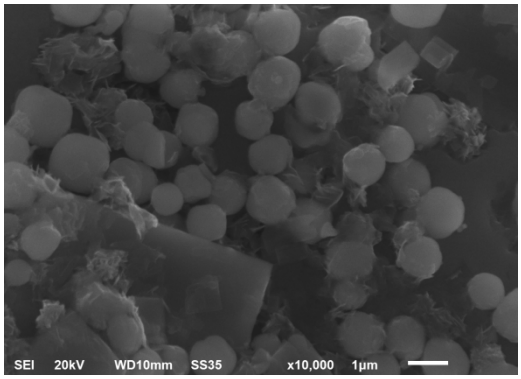


Figure 3. SEM photograph of $Rb_2K_2[\gamma\text{-}H_2SiV_2W_{10}O_{40}].nH_2O$.

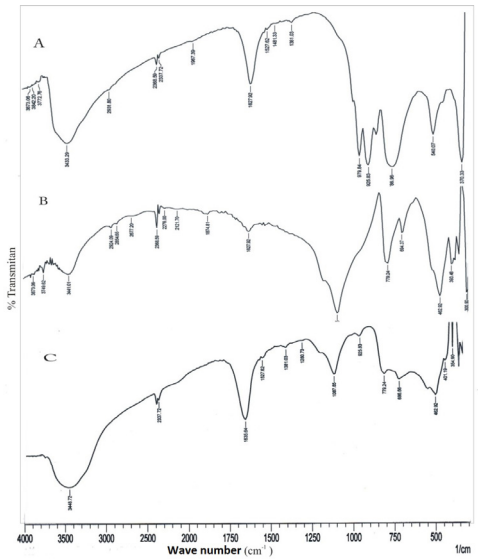


Figure 4. FTIR spectrum of $Rb_2K_2[\gamma\text{-}H_2SiV_2W_{10}O_{40}].nH_2O$ (A), $SiO_2$ (B), and $Rb_2K_2[\gamma\text{-}H_2SiV_2W_{10}O_{40}]$ $.nH_2O/SiO_2$ (C).

compound $Rb_2K_2[\gamma\text{-}H_2SiV_2W_{10}O_{40}].nH_2O$ is needed to support with a metal oxide. Metal oxides such as silica, titanium, zirconium, and also tantalum chloride will be used as a support of $Rb_2K_2[\gamma\text{-}H_2SiV_2W_{10}O_{40}].nH_2O$.

In the first experiment, silica dioxide was used as a support of $Rb_2K_2[\gamma\text{-}H_2SiV_2W_{10}O_{40}].nH_2O$ and the materials were characterized using FTIR analysis as shown in Figure 4.

Figure 4C showed that polyoxometalate $Rb_2K_2[\gamma\text{-}H_2SiV_2W_{10}O_{40}].nH_2O/SiO_2$ has broaden peaks in the wavenumber range 600-1000 $cm^{-1}$, which is attributed from a support agent. Although FTIR spectrum of $Rb_2K_2[\gamma\text{-}H_2SiV_2W_{10}O_{40}].nH_2O/SiO_2$ was broaden but vibration of W-Oc-W and W-Oe-W is still appeared around 900-1000 $cm^{-1}$. That vibrations are clue for silica oxide successfully supported polyoxometalate. Further characterization was conducted using XRD and powder diffractogram is presented in Figure 5.

Diffraction of material $Rb_2K_2[\gamma\text{-}H_2SiV_2W_{10}O_{40}].nH_2O/SiO_2$ as shown in Figure 5C has different with both $Rb_2K_2[\gamma\text{-}H_2SiV_2W_{10}O_{40}]$ $.nH_2O$ and $SiO_2$ as starting materials. Diffraction appeared at 18 deg, 21 deg, 24 deg, and 28 deg. Peaks at 18 deg and 21 deg are probably come from silica and 24 deg, and 28 deg comes from polyoxometalate, which was shifted to lower diffraction. This results indicated increasing crystallinity of material $Rb_2K_2[\gamma\text{-}H_2SiV_2W_{10}O_{40}].nH_2O/SiO_2$. Thus novel properties of $Rb_2K_2[\gamma\text{-}H_2SiV_2W_{10}O_{40}]$ $.nH_2O/SiO_2$ is expected. Further characterization was conducted using SEM. The results identification of morphology using SEM is shown in Figure 6.

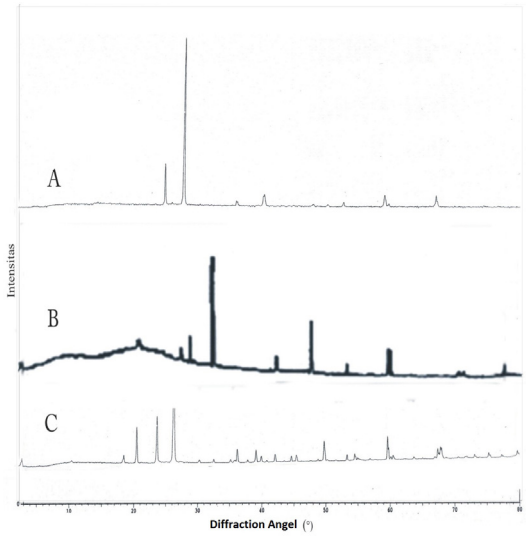


Figure 5. XRD powder pattens of $Rb_2K_2[\gamma\text{-}H_2SiV_2W_{10}O_{40}].nH_2O$ (A), $SiO_2$ (B), and $Rb_2K_2[\gamma\text{-}H_2SiV_2W_{10}O_{40}]$ $.nH_2O/SiO_2$ (C).

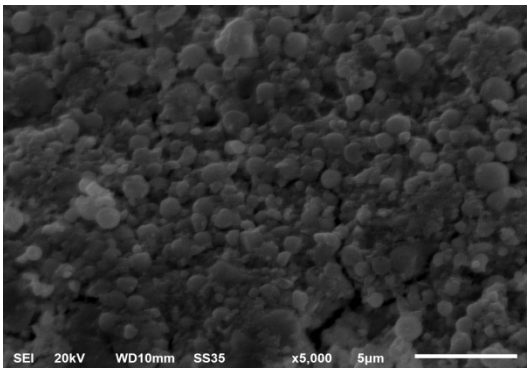


Figure 6. SEM photograph of $Rb_2K_2[\gamma\text{-}H_2SiV_2W_{10}O_{40}].nH_2O/SiO_2$

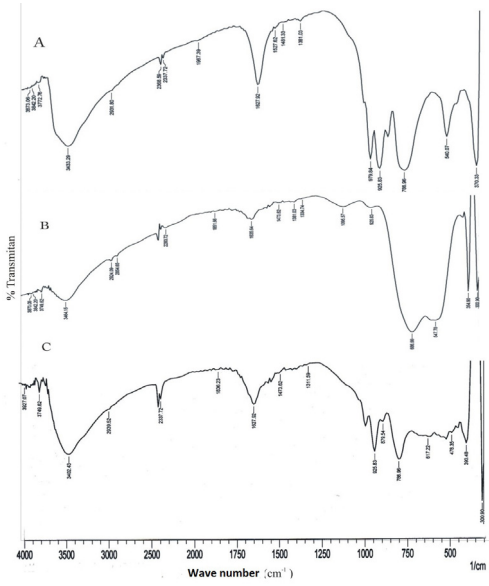


Figure 7. FTIR spectrum of $Rb_2K_2[\gamma\text{-}H_2SiV_2W_{10}O_{40}].nH_2O$ (A), $TiO_2$ (B), and $Rb_2K_2[\gamma\text{-}H_2SiV_2W_{10}O_{40}]$ $.nH_2O/TiO_2$.

Figure 6 showed that material $Rb_2K_2[\gamma\text{-}H_2SiV_2W_{10}O_{40}].nH_2O/SiO_2$ has uniform shape, but small aggregation appeared. Calculation of particle size revealed that material $Rb_2K_2[\gamma\text{-}H_2SiV_2W_{10}O_{40}].nH_2O/SiO_2$ has particle size 2200 nm, which was higher than $Rb_2K_2[\gamma\text{-}H_2SiV_2W_{10}O_{40}].nH_2O$. For comparison of silica oxide as support thus titanium oxide was used as support for Rb-

$_2K_2[\gamma\text{-}H_2SiV_2W_{10}O_{40}].nH_2O$ to form $Rb_2K_2[\gamma\text{-}H_2SiV_2W_{10}O_{40}].nH_2O/TiO_2$. Spectrum FTIR material $Rb_2K_2[\gamma\text{-}H_2SiV_2W_{10}O_{40}].nH_2O/TiO_2$ is presented in Figure 7.

FTIR spectrum in Figure 7C for material $Rb_2K_2[\gamma\text{-}H_2SiV_2W_{10}O_{40}].nH_2O/TiO_2$ looks similar with spectrum FTIR for $Rb_2K_2[\gamma\text{-}H_2SiV_2W_{10}O_{40}].nH_2O/SiO_2$ in Figure 4c. Wavenumber at 700-1000 cm-1 was broad probably due to the interaction of metal oxides both silica and titanium. The vibration of polyoxometalate $Rb_2K_2[\gamma\text{-}H_2SiV_2W_{10}O_{40}].nH_2O/SiO_2$ also appeared at wavenumber in the range 900-1000 $cm^{-1}$, which was attributed to W-Oc-W and W-Oe-W vibrations. Further characterization using XRD toward $Rb_2K_2[\gamma\text{-}H_2SiV_2W_{10}O_{40}].nH_2O/TiO_2$ is shown in Figure 8.

Figure 8 showed XRD powder pattern of $Rb_2K_2[\gamma\text{-}H_2SiV_2W_{10}O_{40}].nH_2O$ (A), $TiO_2$ (B), and $Rb_2K_2[\gamma\text{-}H_2SiV_2W_{10}O_{40}].nH_2O/TiO_2$ (C). Diffraction of $Rb_2K_2[\gamma\text{-}H_2SiV_2W_{10}O_{40}].nH_2O/TiO_2$ as shown in Figure 8C has the main diffraction in the range of 20-30 deg, which was attributed to Titania and polyoxometalate. Another diffraction also appeared at 35-48, 52-57, and 62 deg. This pattern is quite different with silica as support. Probably titanium oxide was dispersed on the surface of polyoxometalate. To know this phenomenon then SEM analysis was conducted and the SEM image of $Rb_2K_2[\gamma\text{-}H_2SiV_2W_{10}O_{40}].nH_2O/TiO_2$ is shown in Figure 9.

SEM photograph in Figure 9 showed although uniform shape appeared, but small aggregation was formed. Calculation of particle size resulted in the size particle 660 nm, which was smaller than polyoxometalate $Rb_2K_2[\gamma\text{-}H_2SiV_2W_{10}O_{40}].nH_2O$ and $Rb_2K_2[\gamma\text{-}H_2SiV_2W_{10}O_{40}].nH_2O/SiO_2$. Titanium and silica have different properties thus the results of support material was also different properties. To know the support properties thus experiment was conducted using zirconium. This experiment used zirconium oxychloride. This support quite different with silica and titanium due to chloride atom include in the support structures. The characterization for compound $Rb_2K_2[\gamma\text{-}H_2SiV_2W_{10}O_{40}].nH_2O/ZrOCl_2$ and starting materials is presented in Figure 10.

The interesting results were found that although zirconium different with silica and titanium but FTIR spectrum is similar to all support in which peaks at wavenumber 700-1000 $cm^{-1}$ is broad. The properties of $Rb_2K_2[\gamma\text{-}H_2SiV_2W_{10}O_{40}].nH_2O/ZrOCl_2$ is then explored through XRD powder pattern as shown in Figure 11.

The results of XRD powder pattern as shown in Figure 11C for $Rb_2K_2[\gamma\text{-}H_2SiV_2W_{10}O_{40}].nH_2O/ZrOCl_2$ indicated that that material has high crystallinity than silica and titanium as support. There are diffraction peaks at several areas i.e. less than 10 deg, 15-18 deg, and 25-33 deg. Diffraction of zirconium and polyoxometalate was overlapped. Diffraction at 8 deg is new diffraction which was probably due to oxide and chloride interaction with polyoxometalate, and this diffraction is not found for silica or titanium as supports. Characterization using SEM for material $Rb_2K_2[\gamma\text{-}H_2SiV_2W_{10}O_{40}].nH_2O/ZrOCl_2$ as shown in Figure 12 is also interesting due to equal portion aggregation and uniform shapes.

Particle size calculation showed that material $Rb_2K_2[\gamma\text{-}H_2SiV_2W_{10}O_{40}].nH_2O/ZrOCl_2$ has particle size 220 nm. This particle size is widely different with polyoxometalate and other supports. To investigate the difference between pure oxides (silica and titanium), mixture oxide (zirconium), thus no oxide was used as support. Tantalum chloride was used as support for polyoxometalate $Rb_2K_2[\gamma\text{-}H_2SiV_2W_{10}O_{40}].nH_2O$ and analysis of FTIR toward $Rb_2K_2[\gamma\text{-}H_2SiV_2W_{10}O_{40}].nH_2O/TaCl_5$ is shown in Figure 13.

FTIR spectrum of $Rb_2K_2[\gamma\text{-}H_2SiV_2W_{10}O_{40}].nH_2O$ (A), and $Rb_2K_2[\gamma\text{-}H_2SiV_2W_{10}O_{40}].nH_2O/TaCl_5$ (B) in Figure 13 showed that similar results were found between oxide, mixture oxide and non-oxide. Wavenumber at 700-1000 $cm^{-1}$ was broad similar with

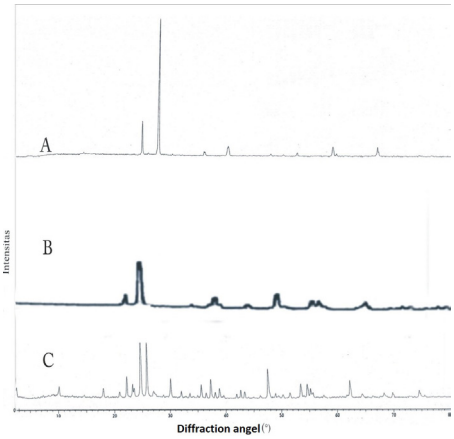


Figure 8. XRD powder patten of $Rb_2K_2[\gamma\text{-}H_2SiV_2W_{10}O_{40}].nH_2O$ (A), $TiO_2$ (B), and $Rb_2K_2[\gamma\text{-}H_2SiV_2W_{10}O_{40}].nH_2O/TiO_2$ (C).

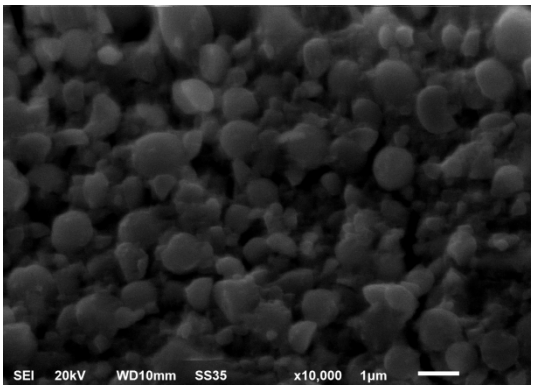


Figure 9. SEM photograph of $Rb_2K_2[\gamma\text{-}H_2SiV_2W_{10}O_{40}].nH_2O/TiO_2$.

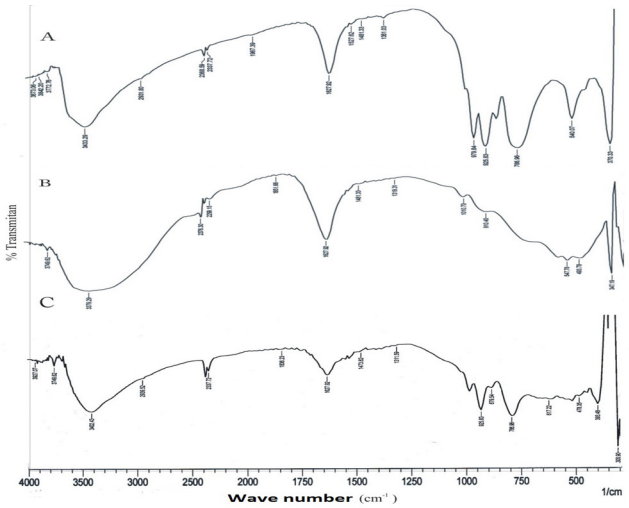


Figure 10. FTIR spectrum of $Rb_2K_2[\gamma\text{-}H_2SiV_2W_{10}O_{40}].nH_2O$ (A), $ZrOCl_2$ (B), and $Rb_2K_2[\gamma\text{-}H_2SiV_2W_{10}O_{40}].nH_2O/ZrOCl_2$.

the use of silica, titanium, and zirconium as supports. Further characterization using XRD and the pattern is shown in Figure 14.

Diffraction of $Rb_2K_2[\gamma\text{-}H_2SiV_2W_{10}O_{40}].nH_2O/TaCl_5$ revealed that there was a sharp peak at diffraction 26 deg and broad peaks at 8-12 deg. This results indicated the use of metal chloride support could create a material with different properties than oxide or mixture oxide supports. Identification using SEM to material $Rb_2K_2[\gamma\text{-}H_2SiV_2W_{10}O_{40}].nH_2O/TaCl_5$ as shown in Figure 15 resulted in particle size 330 nm. This size is smaller than polyoxometalate $Rb_2K_2[\gamma\text{-}H_2SiV_2W_{10}O_{40}].nH_2O$. Thus all experiment shows the dif-

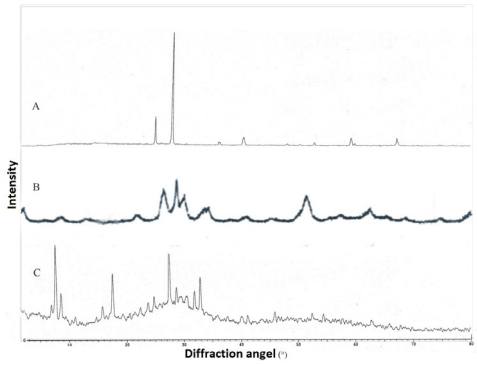


Figure 11. XRD powder patten of $Rb_2K_2[\gamma\text{-}H_2SiV_2W_{10}O_{40}].nH_2O$ (A), $ZrOClO_2$ (B), and $Rb_2K_2[\gamma\text{-}H_2SiV_2W_{10}O_{40}]$ $.nH_2O/ZrOCl_2$ (C).

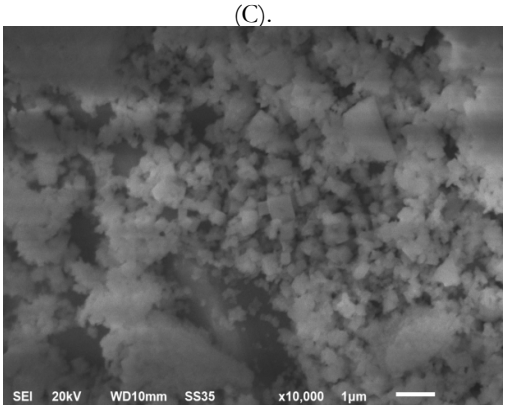


Figure 12. SEM photograph of $Rb_2K_2[\gamma\text{-}H_2SiV_2W_{10}O_{40}]$ $.nH_2O/$ $ZrOCl_2$.

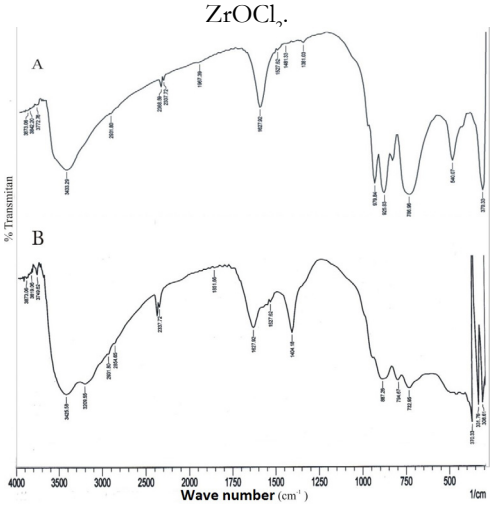


Figure 13. FTIR spectrum of of $Rb_2K_2[\gamma\text{-}H_2SiV_2W_{10}O_{40}]$ $.nH_2O$ (A), and $Rb_2K_2[\gamma\text{-}H_2SiV_2W_{10}O_{40}]$ $.nH_2O/TaCl_5$ (B).

ferent type of supports can create material with unique chemical and physical properties

## CONCLUSION

Metal oxides supported polyoxometalate $Rb_2K_2[\gamma\text{-}H_2SiV_2W_{10}O_{40}].nH_2O$ were successfully conducted using $TiO_2$, $ZrOCl_2$, $TaCl_5$ dan $SiO_2$. The various form and sizes were obtained on supported polyoxometalate with size distribution particles more than 100 nm.

## ACKNOWLEDGEMENT

We thanks to Kemenristekdikti Republik Indonesia for supporting this research through" Hibah Kompetensi" 2015-2016.

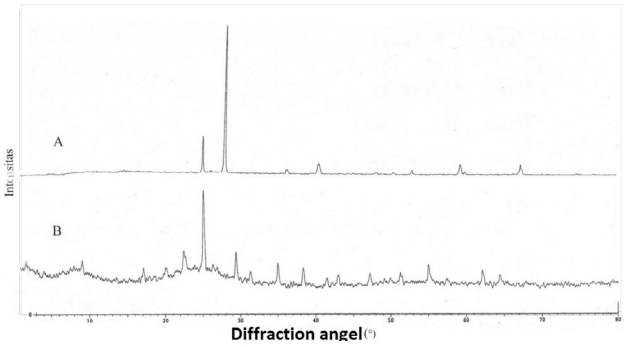


Figure 14. XRD powder patten of $Rb_2K_2[\gamma\text{-}H_2SiV_2W_{10}O_{40}].nH_2O$ (A), and $Rb_2K_2[\gamma\text{-}H_2SiV_2W_{10}O_{40}]$ $.nH_2O/TaCl_5$ (B).

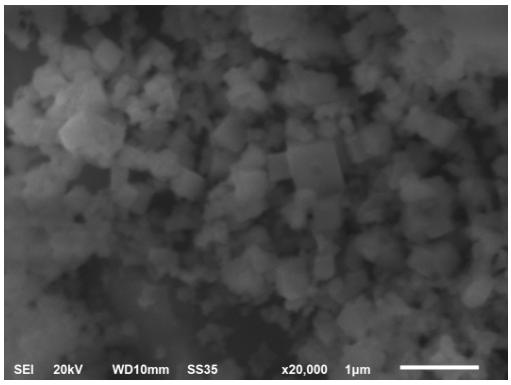


Figure 15. SEM photograph of $Rb_2K_2[\gamma\text{-}H_2SiV_2W_{10}O_{40}].nH_2O/$ $TaCl_5$.

## REFERENCES

Dehghan. R., Anbia. M. (2017). Zeolites For Adsorptive Desulfurization From Fuels: A Review. Fuel Processing Technology, 167, 99-116.

Devassy. B.M, Halligudi. S.B, Hedge. S.G, Halgeri. A.B, Lafebvre. F. (2002). 12-Tungstophosphoric Acid/Zirconia-A Highly Active Stable Solid Acid-Comparison With A Tungstated Zirconia Catalyst. Chemical Communications, 1074-1075.

Dizaji. A.K., Mortaheb. H.R., Mokhtarani. B. (2017). Preparation of Supported Catalyst by Adsorption of Polyoxometalate on Graphene Oxide/Reduced Graphene Oxide. Materials Chemistry and Physics, 199, 424-434.

Gao. Y., Eghtesadi. S.A., Liu. T. (2017). Chapter Two-Supramolecular Structures Formation of Polyoxometalates in Solution Driven by Counterion-Macroion Interaction. Advances in Inorganic Chemistry, 69, 29-65.

Genovese. M., Lian. K. (2017). 6-Polyoxometalates: Molecular Metal Oxide Clusters for Supercapacitors. Metal Oxides in Supercapacitors (A Volume in Metal Oxides), 133-164.

Hanifa. Y., Palapa. N.R. (2016). Mg/Al Double layer Hydroxides: Intercalation with $H_3[\alpha\text{-}PW_{12}O_{40}].nH_2O$. Science and Technology Indonesia, 1, 16-19.

Kim. H. J, Shul. Y. G, and Han. H. (2006). Synthesis of Heteropolyacid $(H_3PW_{12}O_{40})/SiO_2$ Nanoparticles and Their Catalytic Properties. Applied Catalysis A: General, 299, 46-51.

Nakagawa. Y., Mizuno. N. (2007). Mechanism of $[\gamma\text{-}H_2SiV_2W_{10}O_{40}]^{4-}$ Catalyzed Epoxidation of Alkenes with Hydrogen Peroxide. Inorganic Chemistry, 46,5, 1727-1736.

Nakagawa. Y., Uehara. K., Mizuno. N. (2005). Reactivity of Bis(μ-hydroxo)Divanadium Site in $\gamma\text{-}H_2SiV_2W_{10}O_{40}^{4-}$ with Hydroxo Compounds. Inorganic Chemistry, 44, 24, 9068-9075.

Pettinari. C., Pettinari. R., Marchetti. F. (2016). Chapter Four-Gold-

en Jubilee for Scorpionates: Recent Advances in Organometallic Chemistry and Their Role in Catalysis. Advances in Organometallic Chemistry, 65, 175-260.

Pozniczek. J, Lubanska. A, Micek-llnicka. A, Mucha. D, Lalik. E, Bielanski. A. (2006). $TiO_2$ and $SiO_2$ Supparted Well-Dawson Heteropolyacid $H_6PW_{18}O_{62}$ As The Catalyst For ETBA Formation. Applied Catalysis A: General, 298, 217-224.

Ramdass. A., Sathish. V., Babu. E., Velayudham. M., Thanasekaran. P., Rajagopal. S. (2017). Recent Developments on Optical and Electrochemical Sensing of Copper(II) Ion Based on Transition Metal Complexes. Coordination Chemistry Reviews, 343, 278-307.

Tambunan. O.R., Mohadi. R. (2017). Preparation of Polyoxometalate Compound $(NH_4)_6[\beta\text{-}P_2W_{18}O_{62}]/SiO_2$ by Sol Gel Method and Its Characterization. Science and Technology Indonesia, 2, 1-8.

Wang. G., Yang. Y., Han. D., Li. Y. (2017). Oxygen Defective Metal Oxides For Energy Conversion and Storage. NanoToday, 13, 23-39.

Yong. M., Kim. D.S., Lee. T.J., Lee. S.J., Lee. K.G., Choi. B.G. (2016). Polyoxometalate-Grafted Graphene Nanohybrid For Electrochemical Detection of Hydrogen Peroxide and Glucose. Journal of Colloid and Interface Science, 468, 51-56.